PAPER • OPEN ACCESS

Honeybee flight dynamics and pair separation in windy conditions near the hive entrance

To cite this article: Bardia Hejazi *et al* 2023 *New J. Phys.* **25** 093046

IOP Publishing New J. Phys. 25 (2023) 093046 https://doi.org/10.1088/1367-2630/acf8ec

New Journal of Physics
The open access journal at the forefront of physics

Deutsche Physikalische Gesellschaft DPG
IOP Institute of Physics

Published in partnership with: Deutsche Physikalische Gesellschaft and the Institute of Physics

OPEN ACCESS

RECEIVED
29 June 2023

REVISED
4 September 2023

ACCEPTED FOR PUBLICATION
12 September 2023

PUBLISHED
25 September 2023

PAPER

Honeybee flight dynamics and pair separation in windy conditions near the hive entrance

Bardia Hejazi[1,2,*], **Hugo Antigny**[1,3], **Sophia Huellstrunk**[1,4] **and Eberhard Bodenschatz**[1,2,5,6,*]

[1] Laboratory for Fluid Physics, Pattern Formation and Biocomplexity, Max Planck Institute for Dynamics and Self-Organization (MPI-DS), 37077 Göttingen, Germany
[2] Max Planck University of Twente Center for Complex Fluid Dynamics, MPI-DS, 37077 Göttingen, Germany
[3] Universite Grenoble Alpes, Grenoble INP—Phelma, Grenoble 38000, France
[4] Princeton University, Princeton, NJ 08544, United States of America
[5] Institute for Dynamics of Complex Systems, University of Göttingen, 37077 Göttingen, Germany
[6] Laboratory of Atomic and Solid State Physics and Sibley School of Mechanical and Aerospace Engineering, Cornell University, Ithaca 14853, NY, United States of America
[*] Authors to whom any correspondence should be addressed.

E-mail: bardia.hejazi@ds.mpg.de and eberhard.bodenschatz@ds.mpg.de

Keywords: honeybee, insect, flight control, collective behavior

Abstract

Animals and living organisms are continuously adapting to changes in their environment. How do animals, especially those that are critical to their ecosystem, respond to rapidly changing conditions in their environment? Here, we report on the three-dimensional trajectories of flying honeybees under calm and windy conditions in front of the hive entrance. We also investigate the pitch and yaw in our experiments. We find that the mean velocities, accelerations and angular velocities of honeybees increase with increasing wind speeds. We observed that pair separation between honeybees is highly controlled and independent of wind speeds. Our results on the coordination used by honeybees may have potential applications for coordinated flight of unmanned aerial vehicles.

1. Introduction

Animal behavior is influenced by the surrounding environment and changes to the environment. The change in air currents and surface winds impacts the behavior of flying animals, and with the potential increase in wind speeds [1] due to climate change, flying animals may need to adapt their behavior to new conditions. Flying insects such as honeybees are able to adapt to changes in surrounding air flows [2] and maintain flight control even under strongly turbulent conditions [3]. In this work we further explore how honeybees behave and fly in different conditions to better understand their flight dynamics and responses especially when flying in close proximity to one another. The ability for insects to maintain stability and control while in flight [4] and understanding the strategies they use, can aid in improving the systems required for the navigation of small-scale flying robotic collectives [5, 6].

Insects are particularly well suited for research because of their small size, abundance, and the relative ease in which experiments can be carried out on them. Which is why fruit flies have been a long favored example of flying insects for studies [7–10]. Insects also provide us with the exceptional opportunity to study collective behavior, i.e. their group and social dynamics, as demonstrated by studies of swarming midges [11, 12]. Another insect of particular interest is the honeybee (and other species of bees), due to their important ecological role as natural pollinators [13, 14] on the one hand, but also due to their unique social structure. Experiments studying the social behavior and dynamics of honeybees mostly focus on activity at the hive entrance [15–19]. Studies that investigate swarms look at stationary collectives that are not in flight, such as work investigating the mechanical stability of honeybee swarms [20, 21].

Experiments studying honeybee flight are usually carried out in the laboratory and investigate the flight of individuals, focusing on wing aerodynamics [22, 23] and dynamical responses to different air flows

[2, 24]. Although not as numerous as laboratory studies, field experiments have also investigated honeybee flight stability in windy conditions and observe that honeybees increase roll stability by extending their hind legs [25]. More recently, experiments have studied honeybee flight dynamics outside and looking at the trajectories of honeybees near the hive entrance [26], while also considering the influence of turbulence on honeybee flight [3]. However, there is still a lack of research on the collective flight of honeybees and how they avoid collisions with one another mid-flight. Studies suggest that collision avoidance is achieved through visual sensing [27]. Honeybees may also use other senses for navigation and collision avoidance, for instance, it has been shown that honeybees are capable of sensing electric fields [28, 29] and use this to their advantage when foraging [30] while also contributing to atmospheric electric fields when swarming [31]. In this study we examine the flight dynamics and pair statistics of honeybees near the hive entrance, outside in the open where they are free to fly unhindered. We track honeybees using high-speed, high-resolution cameras and investigate their flight and behavior in natural calm weather conditions and compare to conditions where we generate winds with different mean flow velocities.

2. Methods

The experiments were performed at the Max Planck Institute for Dynamics and Self-Organization in Göttingen, Germany. Experiments were performed on 27 July 2022, from 10:00 to 16:00. The ambient temperature during the experiments was between 20 °C–23 °C with no precipitation. Experiments were performed at the entrance of a honeybee hive from the *Apis mellifera carnica* species, as shown in figure 1. Performing experiments in front of the entrance allows us to study landing and take-off dynamics and to additionally examine the interactions between pairs of honeybees mid-flight.

We created wind in front of the hive using a Trotec model TTV 4500 industrial grade fan with a diameter of 42 cm that had three speed settings. The fan generated a uniform and steady supply of air flow where the vector perpendicular to the plane of the fan was approximately at a 45° angle with respect to $-\hat{x}$ and $\hat{y}$ with a slight upwards tilt in the $\hat{z}$ direction. Since the landing platform at the hive entrance was elevated from the ground, the slight upward tilt in $\hat{z}$ allowed for the generated wind to cover the center of our measurement volume. We measured the ambient air flow with no generated wind and the wind speed produced by the fan using a testo 405i thermal anemometer probe. The anemometer accuracy as stated by the manufacturer is $\pm 0.1\ \mathrm{m\,s^{-1}}$ for speeds from 0 to $2\ \mathrm{m\,s^{-1}}$ and $\pm 0.3\ \mathrm{m\,s^{-1}}$ for speeds from 2 to $15\ \mathrm{m\,s^{-1}}$. We measured air flow velocities by placing the probe in the center of the measurement volume before each experiment and removing it before recording videos. We performed experiments under three different wind conditions; no wind (with natural air flows), moderate wind (medium wind speed on the fan), and strong wind (maximum wind speed on the fan). The details of the experimental conditions and wind velocities are given in table 1. The natural air flows were approximately 9% of the moderate and 5% of the strong wind settings of the fan. Thus, the natural air flow was much weaker than the flow produced by the fan.

We recorded images using 4 Phantom VEO4K 990L cameras equipped with 50 mm lenses capturing 4096 $\times$ 2034 pixel images at 200 frames per second with approximately 30 s of continuous image capture before the camera RAM was full and data transfer was initiated. We recorded a total of 25 videos for the no wind and moderate wind conditions and recorded 10 videos for the strong wind conditions. We recorded less videos for strong wind conditions to limit the time we exposed the honeybees to intense winds and to minimize disturbance to the hive. The cameras had different viewing angles which created an effective measurement volume of $60\,(L) \times 70\,(W) \times 30\,(H)$ centimeters. Cameras are triggered and synced using an external signal generator. We used a small pavilion that covered the cameras to protect them from overheating due to direct exposure to the Sun and potential harm from any precipitation that may occur during experimentation. We use two data servers for rapid data transfer of video recordings from the camera RAM. The data servers were mounted on a shockproof rack located in a mobile laboratory. The mobile laboratory is a custom van meant for experiments in the field. The experimentalists were seated in the van while experiments were underway and monitored the image capture and download.

Imaging and tracking of honeybees is based on previous methods and in-house codes used to track honeybees using consumer-grade GoPro cameras [3] and similar high-speed Phantom cameras used to track particles in turbulence experiments [32, 33].

The high-resolution cameras used in these experiments allowed us to clearly image honeybees and all their features. From our images we are able to determine honeybee body orientations using a nonlinear fitting algorithm. The routine optimizes for the honeybee position and orientation by minimizing the difference between a model that is projected onto the camera image plane and the actual honeybee images [32]. An example of the orientation finding process is shown in figure 2. Figures 2(a)–(d) shows the raw images obtained with our four cameras at the same instance in time. The honeybee identified with the green square outline is seen on all four cameras at this frame. Figures 2(e)–(h) shows the zoomed in image of

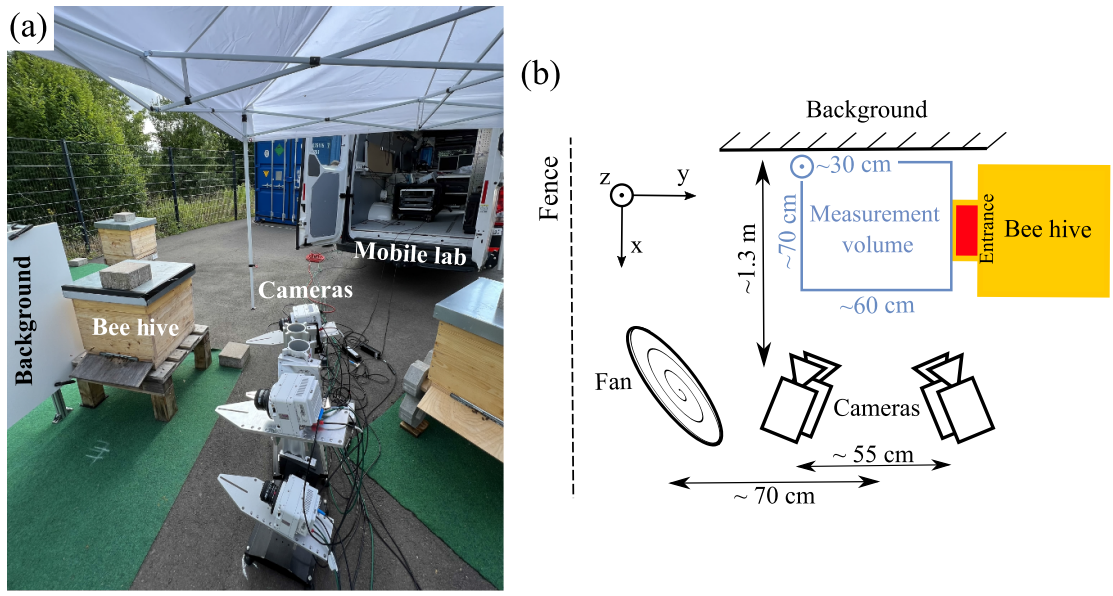

Figure 1. (a) Experimental setup showing the honeybee hive, cameras and background with the overhead shade from the pavilion to protect the cameras from the elements (fan not shown). Also shown is the mobile laboratory where data servers are located and experimentalists monitor recordings. (b) Schematic of the experimental setup showing the location and distances between cameras, background, and fan. The measurement volume in our experiments is approximately $60\,(L) \times 70\,(W) \times 30\,(H)$ centimeters where the length is along $\hat{y}$, the width along $\hat{x}$, and the height along $\hat{z}$.

Table 1. Air flow speed measurements along with the number of video recordings for each experiment setting. The mean flow velocity in the x, y, and z direction is reported, with the total mean flow velocity being U.

Exp.	U_x (m s^{-1})	U_y (m s^{-1})	U_z (m s^{-1})	U (m s^{-1})	No. recordings
No wind	−0.2	0.1	0.05	0.23	25
Moderate wind	−1.0	2.2	0.5	2.46	25
Strong wind	−1.9	4.0	0.6	4.46	10

the honeybee identified in figures 2(a)–(d). We calculated the honeybee orientation using a 3D capsule-like shape. The raw images were background subtracted and inverted resulting in a clear image intensity gradient from honeybee to background. The modeled shape was also given an intensity gradient similar to the actual image of the honeybee for improved optimization. The 3D model was then projected onto the four two-dimensional (2D) image planes and optimized so that the differences in pixel intensity between the actual honeybee image and projected model image was minimized. With this method we were able to find the honeybee orientation as shown in figures 2(i)–(l), where the beginning and end of the projected model image are shown on the actual honeybee image. The honeybee center and reprojected center is also shown to demonstrate the tracking precision. The reprojected center was obtained by reprojecting the 3D stereomatched point, obtained using the honeybee center initially found from the four camera images, back to the 2D camera image plane. Figures 2(m)–(p) show the optimized projection of the model capsule-like shape on the 2D camera image planes at the location of the honeybee identified in the previous figure panes. We should note that from examining the images of honeybees in our experiments, the angle between the honeybee thorax and abdomen does not significantly change during the flights observed here. Therefore, we find that the capsule-like shape used to model the body of a honeybee is a reasonable approximation.

3. Results

We calculated honeybee flight velocities and accelerations using polynomial fits to the three-dimensional (3D) trajectories with fit-length of $h = 7$ where each track of length l is split into $l - 2h$ sections for fitting. As a result, we only analyzed tracks longer than 10 frames or 50 ms. Furthermore, we only used data in the analysis where the stereomatching error was no more than 5 pixels. The resulting mean tracking error across all cameras was approximately one pixel where an individual bee is approximately 4000 pixels in size. Table 2 shows the total number of tracks, mean track length, and maximum track length of each wind condition experiment. We can see that as the wind intensity increases the mean and maximum track lengths decreases, thus honeybees seem to not linger in windy conditions when compared to mild, no wind conditions.

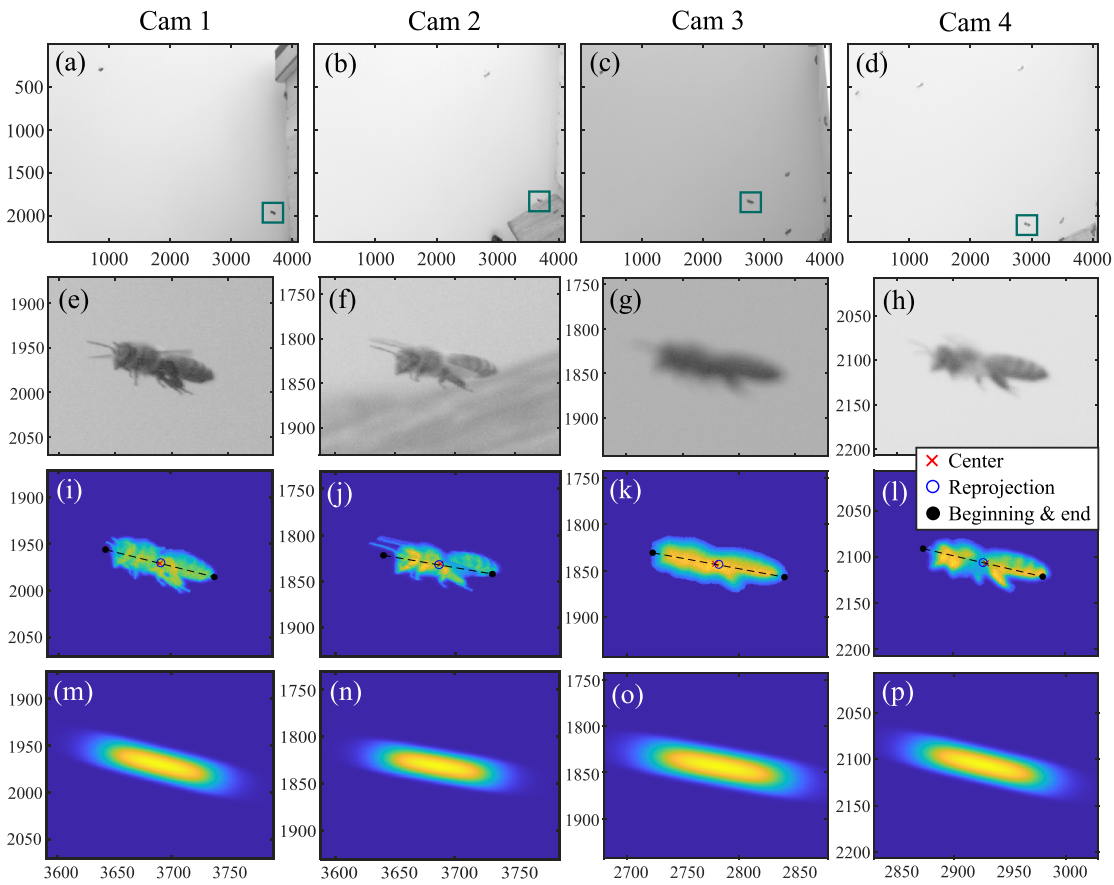

Figure 2. Example of honeybee orientation finding procedure. (a)–(d) raw images from the cameras at the same frame number where an identified honeybee is seen on all four cameras and is tracked. (e)–(h) Zoomed in image of the identified honeybee in (a)–(d). (i)–(l) Background subtracted and processed image of the honeybee where the center, beginning, and end of the honeybee are identified by fitting a capsule-like shape to the honeybee. (m)–(p) The capsule model that is fitted to the honeybee at the same position as the honeybee in (i)–(l).

Table 2. The total number of tracks, mean track length, and maximum track length for each experiment setting.

Exp.	No. tracks	Mean track length	Max. track length
No wind	3894	59	504
Moderate wind	3948	43	459
Strong wind	797	37	272

Figure 3 shows the probability distribution function (PDF) of the honeybee velocity and acceleration components in different wind conditions. From figures 3(a), (c) and (e), we observe an unsymmetrical pattern in the velocity component PDF's. Here when there is no wind generated by the fan (blue filled circles), the honeybee has larger velocities when leaving the hive as shown by the skewed PDF of v_y towards larger negative values. While, the other two components of v_x and v_z remain symmetric. However, as we introduced wind, the velocity component PDF's changed in that the honeybee velocity is skewed in the same direction as the mean wind velocity for all components of v. The acceleration components do not show strong signs of asymmetry but as the wind intensity increases, the mean acceleration magnitude also increases, this is also the case for the mean honeybee velocity magnitude. The mean honeybee velocity and acceleration magnitudes in different wind conditions are given in table 3.

Figure 4 shows the PDF of the honeybee flight power per insect mass, defined as $P = a \cdot v'$, where $v' = v_b - v_w$, is obtained by subtracting the mean wind velocity from the honeybee velocity. Here we assume that the mass difference between honeybees is negligible as compared to the variance in their velocity and acceleration. We calculate the flight power using definitions from Lagrangian turbulence used to determine the change in kinematic energy of tracer particles advected in turbulent flow [34]. We can estimate the power needed by a honeybee to overcome the aerodynamic drag in windy conditions by multiplying the drag force by the honeybee velocity, $P_d = F_d\, v_b$. To obtain an upper-bound for P_d we calculate the power needed if the honeybee were to fly in headwind using the relation $P_d = \frac{1}{2} C_d A \rho (v_w + v_b)^2 v_b$. Here C_d is the dimensionless

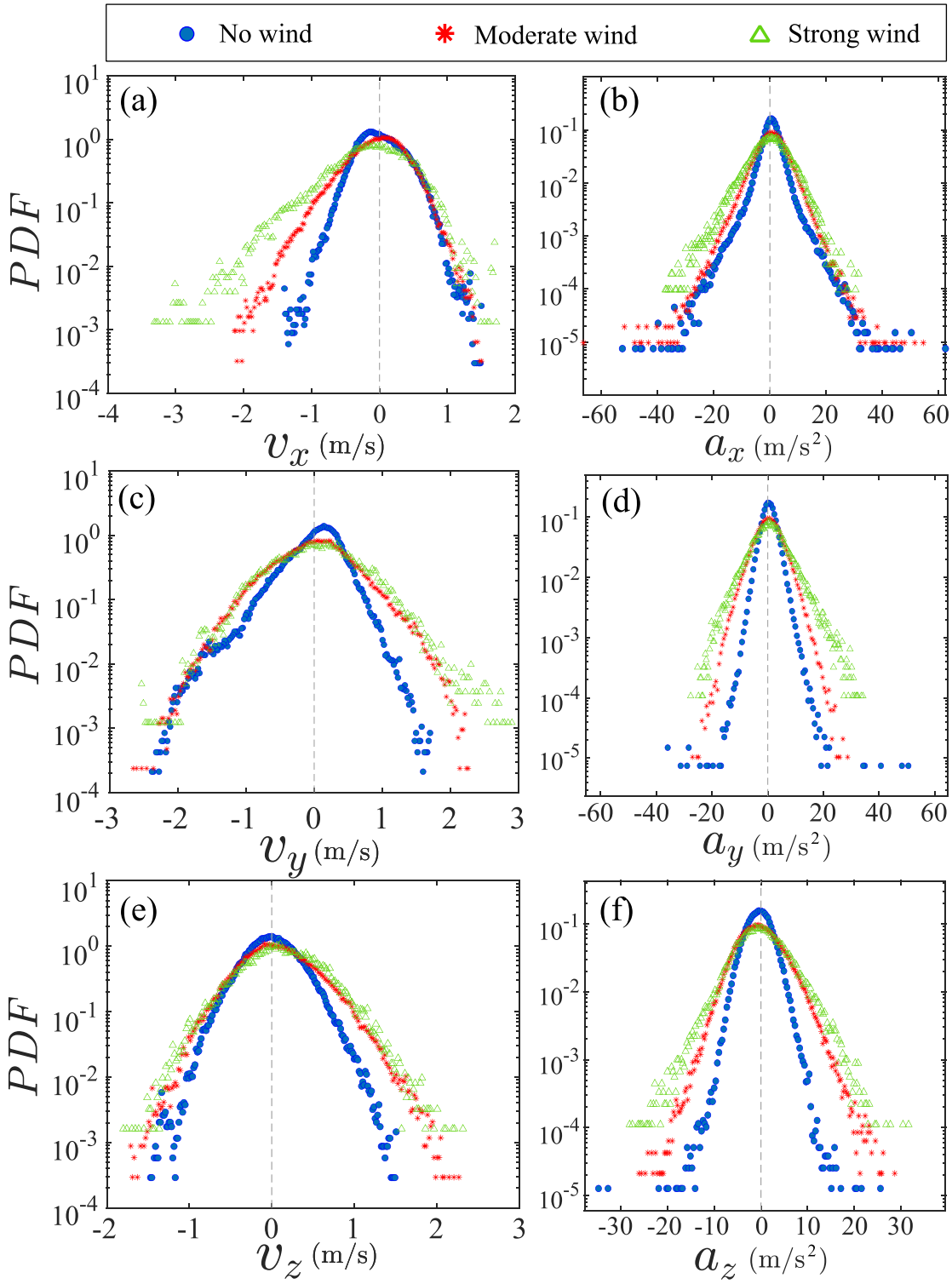

Figure 3. The probability distribution function (PDF) for honeybee velocity and acceleration components in different wind conditions. (a), (b) x components, (c), (d) y components, and (e), (f) z components. The mean velocity and accelerations increase with wind strength. The mean wind direction is in the $+y$, $-x$, and $+z$ direction.

drag coefficient, A is the cross-sectional area of the object, and ρ is the fluid density. We use the mean values reported in tables 1 and 3 for the wind and honeybee velocities respectively. Furthermore, we use $\rho \approx 1.2\,\mathrm{kg\,m^{-3}}$ for air at 20 °C, and a 2 cm sphere for the approximation of the cross-sectional area of a honeybee given that the average honeybee has a body length and wingspan of just under 2 cm [35]. Experiments have shown that a value of $C_d = 0.5$ is an appropriate estimate of the honeybee drag coefficient for the wind speeds investigated in this study [36]. Using these values and given that the average honeybee weighs approximately 100 mg [37], we can calculate the power needed to overcome aerodynamic drag per

Table 3. The mean velocity, acceleration, and power magnitudes for each wind condition experiment ± the standard deviation.

Exp.	$\langle \lvert v \rvert \rangle$ (m s^{-1})	$\langle \lvert a \rvert \rangle$ (m s^{-2})	$\langle \lvert P \rvert \rangle$ (m^2 s^{-3})
No wind	0.53 ± 0.27	4.52 ± 2.88	1.24 ± 1.55
Moderate wind	0.72 ± 0.38	7.58 ± 4.11	10.01 ± 9.22
Strong wind	0.86 ± 0.46	9.43 ± 5.42	25.03 ± 23.99

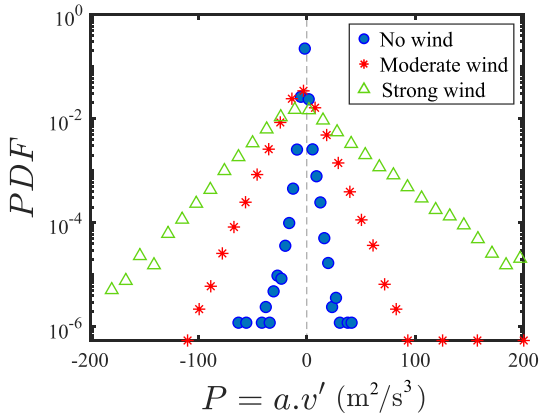

Figure 4. The PDF of honeybee flight power, $P = a \cdot v'$, for different wind conditions. The mean flight power is increasing with mean wind velocity to overcome the increasing aerodynamic drag.

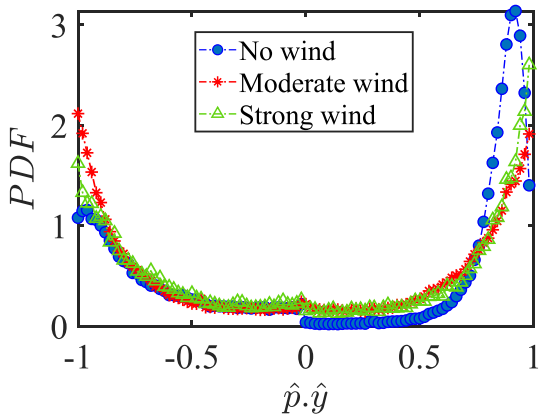

Figure 5. The cosine of the angle between the honeybee body vector, $\hat{p}$, and the global $\hat{y}$ vector for different wind conditions. $\hat{p} \cdot \hat{y} > 0$ shows instances where the honeybee is facing towards the hive and is generally moving towards the hive and $\hat{p} \cdot \hat{y} < 0$ is for when the honeybee is facing away from the hive and is generally moving away from the hive.

unit mass to be between approximately 30 m^2 s^{-3} at moderate wind strengths and 100 m^2 s^{-3} in strong winds. This increase in flight power needed by a honeybee to overcome the aerodynamic drag, from flying in no wind conditions to flying in windy conditions, is demonstrated in figure 4. It is also interesting to note that in windy conditions the flight power appears to be intermittent and follows an exponential distribution.

Similarly to the mean velocity and acceleration magnitudes, the mean flight power magnitude also increases with increased wind velocity. In previous work we had observed that the mean flight performance of honeybees ($\langle \lvert v \rvert \rangle$, $\langle \lvert a \rvert \rangle$, and $\langle \lvert P \rvert \rangle$) did not change as we changed the wind turbulence intensity [3]. In our previous experiments the mean wind velocity did not change significantly and was approximately uniform for all turbulence intensities investigated. However, now by significantly changing the mean wind velocity we clearly see a dependence of the flight performance on wind intensity.

Performing experiments in front of the hive entrance also allows us to investigate landing and takeoff dynamics. Figure 5 shows the cosine of the angle between the honeybee body vector, $\hat{p}$, and the horizontal axis $\hat{y}$. The vector that defines the honeybee body orientation is the vector that lies along the length of the honeybee body from the tail to head or end to beginning of the honeybee as shown in figures 2(i)–(l). When $\hat{p} \cdot \hat{y} > 0$, the honeybee is facing towards the hive and is generally flying towards the hive. Similarly, when $\hat{p} \cdot \hat{y} < 0$, the honeybee is facing away from the hive and is generally flying away from the hive. The reason we

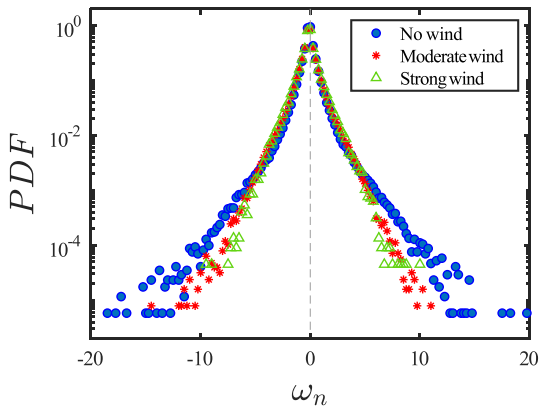

Figure 6. The PDF of honeybee angular velocity in different wind conditions. Here the angular velocity is calculated based on the pitch and yaw angles. The mean of angular velocities increases with mean wind velocity.

use the term generally is that occasionally when the hive entrance was crowded the honeybees hovered or flew backwards away from the hive while facing towards the hive. The honeybees seemingly have a preferential body orientation while they fly away and towards the hive in no wind conditions, as can be seen by the maxima in the PDF of the cosines. In no wind conditions, the honeybees have larger angles away from the horizontal as they approach the hive in anticipation of landing as compared to when leaving the hive with larger velocities (figure 3(c)). However, this preferential body angle while flying disappears when we introduce wind and the honeybees prefer to fly in a way that their body is mostly horizontal and aligned with $\hat{y}$. Further investigation is needed to determine why a more horizontal flight is preferred in windy conditions and if it causes increased flight stability in windy and unstable conditions. The slight discontinuity at $\hat{p}\cdot\hat{y}=0$ is caused by the preferred flight path of the honeybees due to the experimental setup and the surrounding environment. As shown in figure 1, the fencing and background influence the honeybees to fly in the $\hat{x}$ and $-\hat{y}$ direction when flying away from the hive, which corresponds to the larger probability of negative $\hat{p}\cdot\hat{y}$ values around zero. It is also worth noting that in no wind conditions (blue filled circles), we observed more honeybees flying towards the hive than flying away from the hive, an approximately 60 to 40 percent split in the data. This may be due to the busy nature of the hive entrance and the need for honeybees to find a clear opening for landing. The moderate and strong wind conditions however had an even split between honeybees leaving and approaching the hive which may be caused by an increased back and forth flight due to less flight control.

We calculated the honeybee angular velocity from the honeybee body orientation. Figure 6 shows the PDF of the honeybee angular velocity where $\omega_n=(1/3)(P(\omega_x/\omega_x')+P(\omega_y/\omega_y')+P(\omega_z/\omega_z'))$, and ω_i' is the standard deviation of ω_i. The angular velocity does not represent the complete angular dynamics of the honeybee since with our orientation finding method we can only obtain two of the three flight angles. The angular velocity shown in figure 6 represents the changes in the pitch and yaw of the honeybee and does not include roll dynamics. Even so, we can still observe interesting dynamics where just as before for the other flight parameters, the mean angular velocity increases with wind mean flow velocity. Table 4 shows the values for the mean angular velocity magnitudes for each wind condition experiment.

An advantage of performing experiments in front of the hive entrance is the ability to image multiple honeybees simultaneously, from which pair statistics can be obtained. In our experiments we were able to image anywhere from at least two to upwards of ten or more honeybees in the same frame. This allowed us to obtain pair statistics such as relative distances, velocities, and accelerations between pairs of honeybees. Figure 7 shows the PDF of the distance between every two honeybees seen at the same instance in time. While honeybees appear to have less control in their flight in windy conditions, since all other flight parameters (v, a, P, and ω) were affected by the change in wind speed, the pair separation, r, is not influenced and honeybees maintain a constant distance from one another independent of the wind intensity. The mean pair separations for all wind conditions are also given in table 4. We should note however, that the mean pair separations are most likely specific to the experimental conditions reported here and are likely dependent on the number density of bees flying in the measurement volume and the size of the measurement volume itself. For instance, due to the influence of the measurement volume, the probability of finding honeybees at a particular r decreases as r increases.

Figure 8 shows the relative velocity and acceleration magnitudes between pairs of honeybees as a function of their separation distance r. Here, $v_{\mathrm{rel}}=v_1-v_2$ and $a_{\mathrm{rel}}=a_1-a_2$ are the vector differences between the

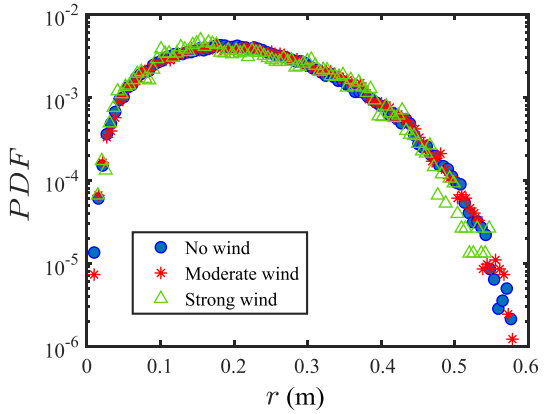

Figure 7. The PDF of the distance between every pair of honeybees seen at the same instance in time for different wind conditions. Honeybees display the same behavior and maintain a constant distance from one-another in all wind conditions.

Table 4. The mean angular velocity magnitudes and pair separations for each wind condition experiment ± the standard deviation.

Exp.	$\langle\lvert\omega\rvert\rangle$ (rad s^{-1})	r (m)
No wind	4.49 ± 5.03	0.21 ± 0.095
Moderate wind	8.58 ± 8.15	0.22 ± 0.096
Strong wind	10.01 ± 8.84	0.21 ± 0.096

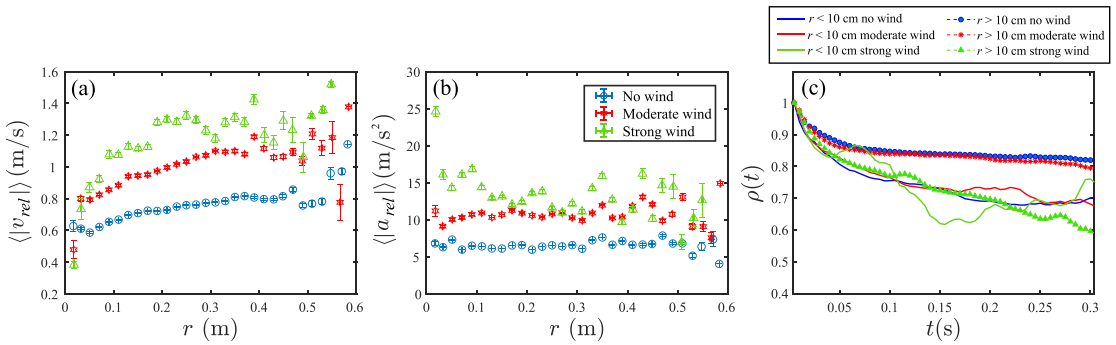

Figure 8. (a) The relative velocity (b) and acceleration magnitudes between pairs of honeybees as a function of their pair separation r. The honeybees have similar velocities to one-another at small separations which increases with separation distance. The relative acceleration is not dependent on r. The error bars show the standard error. (c) The relative acceleration correlation function. Nearer honeybees adjust their velocities more frequently where their relative acceleration decorrelates faster as compared to far away honeybees.

velocities and accelerations of honeybees 1 and 2. $\langle|v_{\rm rel}|\rangle$ and $\langle|a_{\rm rel}|\rangle$ at a given r were calculated by taking the mean of all relative value magnitudes in that given range of r. From figure 8(a) we see that $\langle|v_{\rm rel}|\rangle$ increases with r, meaning that as honeybees approach one-another their velocities are increasingly similar, both in direction and magnitude, since a value of zero represents equal and aligned vectors. In our experiments this behavior may be caused by flight near the hive entrance where honeybees are more likely to be closer to each other near the entrance and fly with similar velocities to land or takeoff. However, $\langle|a_{\rm rel}|\rangle$ remains relatively constant across all separation distances and does not show dependence on r as seen in figure 8(b).

The observation from figures 8(a) and (b) implies that honeybees are seemingly adjusting their velocities more frequently the nearer they are to each other according to the velocities of their nearest neighbors. An implication to this is that the correlation function of the relative acceleration decorrelates faster for neighboring honeybees as compared to far away honeybees. Figure 8(c) shows the relative acceleration correlation times for honeybees near to each other ($r < 10$ cm) and honeybees far away from each other ($r > 10$ cm) for all wind conditions, where the correlation function is defined as $\rho(t) \equiv \langle|a_{\rm rel}(t_0)||a_{\rm rel}(t_0+t)|\rangle / \langle|a_{\rm rel}(t_0)|^2\rangle$. The correlation function for no wind and moderate wind conditions does indeed decorrelate sooner when honeybees are nearer to each other. However, for strong wind conditions, the correlation functions are quite similar for both near and far away honeybees, which is

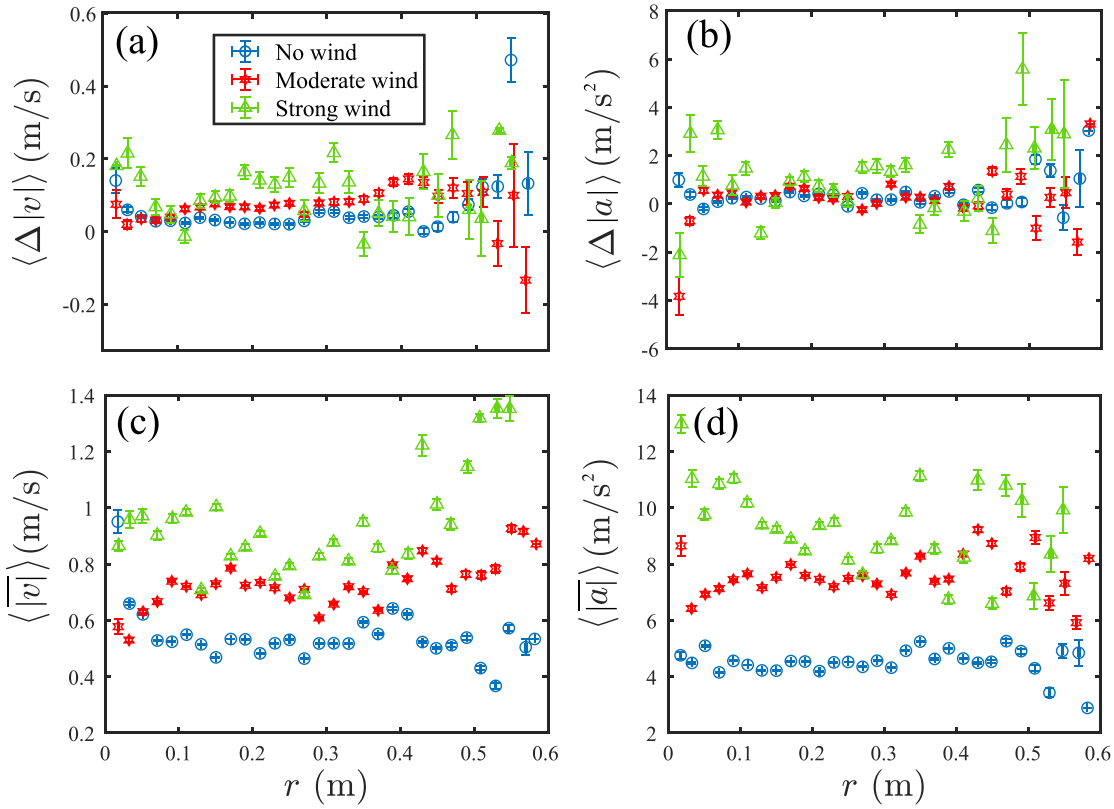

Figure 9. (a) The velocity magnitude difference (b) and acceleration magnitude difference between pairs of honeybees as a function of pair separation.(c) The mean velocity magnitude (d) and mean acceleration magnitude of pairs of honeybees as a function of their separation distance. The honeybees fly with the same average velocity over all separation distances. The error bars show the standard error.

possibly due to the need for honeybees to continuously adjust their flight in more unstable conditions independent of their separation distance.

Figures 9(a) and (b) show the velocity and acceleration magnitude differences between pairs of honeybees as a function of r. The velocity and acceleration magnitude differences are mostly small for all wind conditions meaning that on average the honeybees fly with the same velocity and acceleration magnitudes independent of their separation distance. This is further shown in figures 9(c) and (d) which shows the mean velocity and acceleration magnitudes of pairs of honeybees as a function of r. The mean values for the velocity and acceleration magnitudes remain almost constant over all separation distances and are similar to the mean values reported in table 3 which also increase with increasing wind strength.

4. Conclusions

The mean honeybee velocity, acceleration, flight power, and angular velocity were all influenced by the mean wind velocity where the mean magnitude of all the quantities measured increased with the mean wind velocity. In previous work we had observed at constant mean wind magnitudes that the measured quantities were not dependent on the turbulence intensities [3]. Thus we conclude that it is the mean wind and not the turbulence intensity to which the honey bees respond by changing these properties. In calm no wind conditions the honeybees have a preferential orientation in which they approach and leave the hive. The approach angle is larger than the leaving angle. With wind the honeybees align their bodies with the horizontal axis. Such behavior is perhaps a way to increase flight stability in windy conditions. The limitation to our orientation finding method is that we can only identify two of the three flight angles, namely we can only measure changes in the pitch and yaw. In future work we will also measure roll dynamics with the use of more advanced computer vision techniques [38]. By performing experiments in front of the hive entrance we explored the interaction between individual honeybees. We found that the honeybees maintained a constant distance from one another during flight for all wind conditions. This distance was kept approximately constant even under extreme wind conditions while the honeybees had to adjust other flight parameters such as velocity and acceleration. Furthermore, we observed that honeybees adjust their velocities more frequently the nearer they are to each other according to their nearest neighbors velocity. Future work would need to

further explore pair separations in more detail and investigate under what conditions the pair separation between honeybees can be influenced. Possible avenues of study could be by investigating swarming events and how pair separations are dependent on different number densities of honeybees or by perhaps introducing electric fields and investigating whether such external fields disrupt navigation and collision avoidance. The results presented here on honeybee flight in extreme winds and how their flight is affected, from their body orientation to their pair separation, can aid the improvement of flight stability and control of unmanned flying robots, and the advancement of collision avoidance systems for the coordinated flight of collective robotics.

Data availability statement

The data cannot be made publicly available upon publication because they are not available in a format that is sufficiently accessible or reusable by other researchers. The data that support the findings of this study are available upon reasonable request from the authors.

Acknowledgments

We would like to thank the referees for their invaluable feedback that helped improve this work. The work presented here would not have been possible without the support of the technical staff at the MPI-DS. The authors would like to thank the biology staff for taking care of the honeybee hives. We would like to thank the experimental technicians for help with setting up the mobile laboratory and pavilion. Additionally, many thanks to the IT and HPC team for the setup of the data servers for file transfer and storage. We would like to express our sincere gratitude to Alain Pumir for insightful discussions.

Author contributions

B H planning and development of research project. B H, H A, and S H performing experiments and initial orientation analysis. B H analysis of data and writing original draft. B H, H A, S H, and E B editing and preparation of final draft.

Funding

We would like to thank the Max-Planck-Gesellschaft for support of this work.

Ethics statement

According to the representative for animal experiments in basic research at the Max Planck Society, no ethical or legal statements are required for the experiments presented in this work.

Conflict of interest

The authors declare no competing interests

ORCID iDs

Bardia Hejazi https://orcid.org/0000-0002-9262-128X
Eberhard Bodenschatz https://orcid.org/0000-0002-2901-0144

References

[1] Zeng Z *et al* 2019 A reversal in global terrestrial stilling and its implications for wind energy production *Nat. Clim. Change* **9** 979–85
[2] Crall J D, Chang J J, Oppenheimer R L and Combes S A 2017 Foraging in an unsteady world: bumblebee flight performance in field-realistic turbulence *Interface Focus* **7** 20160086
[3] Hejazi B, Küchler C, Bagheri G and Bodenschatz E 2022 Honeybees modify flight trajectories in turbulent wind *New J. Phys.* **24** 113010
[4] Sun M 2014 Insect flight dynamics: stability and control *Rev. Mod. Phys.* **86** 615–46
[5] Srinivasan M V 2011 Honeybees as a model for the study of visually guided flight, navigation and biologically inspired robotics *Physiol. Rev.* **91** 413–60
[6] Farrell Helbling E and Wood R J 2018 A review of propulsion, power and control architectures for insect-scale flapping-wing vehicles *Appl. Mech. Rev.* **70** 010801
[7] Harrington M 2014 Fruit flies in space *Lab Animal* **43** 3

[8] Vogel S 1966 Flight in *Drosophila*: I. Flight performance of tethered flies *J. Exp. Biol.* **44** 567–78
[9] Buckminster Fuller S, Straw A D, Peek M Y, Murray R M and Dickinson M H 2014 Flying *Drosophila* stabilize their vision-based velocity controller by sensing wind with their antennae *Proc. Natl Acad. Sci.* **111** 1182–91
[10] Manuel Ortega-Jiménez V and Combes S A 2018 Living in a trash can: turbulent convective flows impair *Drosophila* flight performance *J. R. Soc. Interface* **15** 20180636
[11] Attanasi A *et al* 2014 Collective behaviour without collective order in wild swarms of midges *PLoS Comput. Biol.* **10** 1–10
[12] Feng Y and Ouellette N T 2023 Non-uniform spatial sampling by individuals in midge swarms *J. R. Soc. Interface* **20** 20220521
[13] James Hung K-L, Kingston J M, Albrecht M, Holway D A and Kohn J R 2018 The worldwide importance of honey bees as pollinators in natural habitats *Proc. R. Soc.* B **285** 20172140
[14] Delaplane K S, Mayer D R and Mayer D F 2000 *Crop Pollination by Bees* (CABI) (https://doi.org/10.1079/9780851994482.0000)
[15] Butler C G and Free J B 1952 The behaviour of worker honeybees at the hive entrance *Behaviour* **4** 262–92
[16] Magnier B, Ekszterowicz G, Laurent J, Rival M and Pfister F 2018 Bee hive traffic monitoring by tracking bee flight paths *13th Int. Joint Conf. on Computer Vision, Imaging and Computer Graphics Theory and Applications (Funchal, Madeira, Portugal, 27–29 January 2018)* vol 5 pp 563–71
[17] Nha Ngo T, Wu K-C, Yang E-C and Lin T-T 2019 A real-time imaging system for multiple honey bee tracking and activity monitoring *Comput. Electron. Agric.* **163** 104841
[18] Chiron G, Gomez-Krämer P and Ménard M 2013 Detecting and tracking honeybees in 3D at the beehive entrance using stereo vision *EURASIP J. Image Video Process.* **2013** 59
[19] Babic Z, Pilipovic R, Risojevic V and Mirjanic G 2016 Pollen bearing honey bee detection in hive entrance video recorded by remote embedded system for pollination monitoring *ISPRS Ann. Photogramm. Remote Sens. Spat. Inf. Sci.* III **7** 51–57
[20] Shishkov O, Chen C, Allison Madonna C, Jayaram K and Peleg O 2022 Strength-mass scaling law governs mass distribution inside honey bee swarms *Sci. Rep.* **12** 17388
[21] Peleg O, Peters J M, Salcedo M K and Mahadevan L 2018 Collective mechanical adaptation of honeybee swarms *Nat. Phys.* **14** 1193–8
[22] Ahmed I, Abramson C I and Faruque I A 2022 Honey bee flights near hover under ethanol-exposure show changes in body and wing kinematics *PLoS One* **17** 1–15
[23] Altshuler D L, Dickson W B, Vance J T, Roberts S P and Dickinson M H 2005 Short-amplitude high-frequency wing strokes determine the aerodynamics of honeybee flight *Proc. Natl Acad. Sci.* **102** 18213–8
[24] Jakobi T, Kolomenskiy D, Ikeda T, Watkins S, Fisher A, Liu H and Ravi S 2018 Bees with attitude: the effects of directed gusts on flight trajectories *Biol. Open* **7** bio034074
[25] Combes S A and Dudley R 2009 Turbulence-driven instabilities limit insect flight performance *Proc. Natl Acad. Sci.* **106** 9105–8
[26] Mahadeeswara M Y and Srinivasan M V 2018 Coordinated turning behaviour of loitering honeybees *Sci. Rep.* **8** 16942
[27] Groening J, McLeod L, Liebsch N, Schiffner I and Srinivasan M V 2012 When left is right and right is wrong: collision avoidance in honeybees *Frontiers Behav. Neurosci.* **235**
[28] Greggers U, Koch G, Schmidt V, Dürr A, Floriou-Servou A, Piepenbrock D, Göpfert M C and Menzel R 2013 Reception and learning of electric fields in bees *Proc. R. Soc.* B **280** 20130528
[29] Sutton G P, Clarke D, Morley E L and Robert D 2016 Mechanosensory hairs in bumblebees (*Bombus terrestris*) detect weak electric fields *Proc. Natl Acad. Sci.* **113** 7261–5
[30] Clarke D, Whitney H, Sutton G and Robert D 2013 Detection and learning of floral electric fields by bumblebees *Science* **340** 66–69
[31] Hunting E R, O'Reilly L J, Giles Harrison R, Manser K, England S J, Harris B H and Robert D 2022 Observed electric charge of insect swarms and their contribution to atmospheric electricity *iScience* **25** 105241
[32] Hejazi B, Krellenstein M and Voth G A 2019 Using deformable particles for single-particle measurements of velocity gradient tensors *Exp. Fluids* **60** 153
[33] Hejazi B 2021 Particle-turbulence interactions *PhD Thesis* Wesleyan University (https://doi.org/10.14418/wes01.3.125)
[34] Xu H, Pumir A, Falkovich G, Bodenschatz E, Shats M, Xia H, Francois N and Boffetta G 2014 Flight-crash events in turbulence *Proc. Natl Acad. Sci.* **111** 7558–63
[35] Sauthier R, I'Anson Price R and Grüter C 2017 Worker size in honeybees and its relationship with season and foraging distance *Apidologie* **48** 234–46
[36] Nachtigall W and Hanauer-Thieser U 1992 Flight of the honeybee *J. Comp. Physiol.* B **162** 267–77
[37] Holst N and Meikle W G 2018 Breakfast canyon discovered in honeybee hive weight curves *Insects* **9** 176
[38] Mathis A, Mamidanna P, Cury K M, Abe T, Murthy V N, Weygandt Mathis M and Bethge M 2018 DeepLabCut: markerless pose estimation of user-defined body parts with deep learning *Nat. Neurosci.* **21** 1281–9